http://ansinet.com/itj

ITJ

ISSN 1812-5638

INFORMATION TECHNOLOGY JOURNAL

ANSInet
Asian Network for Scientific Information
308 Lasani Town, Sargodha Road, Faisalabad - Pakistan

Information Technology Journal 9 (5): 899-908, 2010
ISSN 1812-5638

Early Fire Detection Based on Flame Contours in Video

Xiao-Lin Zhou, Fa-Xin Yu, Yu-Chun Wen, Zhe-Ming Lu and Guang-Hua Song
School of Aeronautics and Astronautics, Zhejiang University, Hangzhou, China

Abstract: This study proposed a method for early fire detection in video based on flame contours. The whole fire detection process includes three parts, i.e., candidate fire frame selection, flame region selection and flame contour-based fire decision. In the first step, the suspicious frames are detected and the unlikely frames are removed based on frame selection rules. The second step detects the flame pixels in the candidate fire frames by flame region selection rules. In the last step, four operations (i.e., dilation, erosion, mini region erasing and Canny edge detection) are performed on all flame regions to obtain the exact flame contours and then fire decision rules based on three characteristics (i.e., area, perimeter and roundness of flame contours) are employed to determine whether a fire occurs in the video or not. The proposed approach was tested with several video clips in different environments and the experimental results demonstrated its effectiveness.

Key words: Automatic fire detection, dilation and erosion, mini region erasing, canny edge detector, flame features

INTRODUCTION

Fire disasters will cause severe damage to human properties and bring terrible mental and physical injury to us if they cannot be detected and extinguished in time. In the past decades, various sensors, such as humidity sensors, temperature sensors and smoke sensors, have been used to detect and forecast the fire disaster. They were widely used in the past while currently are no longer paid much attention to because of their shortcomings as bellow. First, they sometimes lead to high missing alarm rates because of the lack of intuitionistic fire information. Second, they can only reach a limited range of observation. Furthermore, the fire alarm cannot be sent out immediately if the sensors are far from the fire and the size, the location and the growing rate of the fire can't be provided either (Jin and Zhang, 2009; Zhang *et al*., 2008a; Yuan *et al*., 2009). Therefore, to provide more useful information about fires, many vision-based early fire detection methods emerge with the rapid development of video technology which is widely used in many fields (Xiang-Wei *et al*., 2009a, b; Jin and Zhang, 2009) and are receiving more and more attention from the researchers (Phillips *et al*., 2000; Xu and Xu, 2007) as time goes by.

Recently, many new vision-based methods have been proposed to detect fires in many environments such as home, office, park, forest and so on. Color and motion information are often used for early fire detection (Healey *et al*., 1993). Because the color attribute is one of the most intuitionistic and prominent features of flames, many fire detection schemes based on color information have been proposed. For example, Cho *et al*. (2008) presented a flame detection method based on RGB and HSI color spaces, Jin and Zhang (2009) introduced a fancy method based on the HSI (Hue, Saturation and Intensity) color space to extract the fire-like moving region, Horng *et al*. (2005) offered a fire flame character based on the HSI color space and Celik *et al*. (2007) proposed a fire pixel detection approach based on the YCbCr color space. On the other hand, some recent studies (Toreyin *et al*., 2005, 2006; Chen *et al*., 2004; Phillips *et al*., 2000) have presented several methods to detect fires based on the motion features of flames. For example, Toreyin *et al*. (2006) detected quasi-periodic behavior in flame boundaries using temporal wavelet transform and color variations in flame regions by computing the spatial wavelet transform of moving fire-colored regions. Certainly, color and motion information can be combined to get a better detection performance, for example, in Yu *et al*. (2008) work, they first found rough fire-colored regions based on the RGB color feature and then improved the fire detection performance according to the movement characteristic of the early fire. Furthermore, some vision-based methods discovered fires in video by detecting the smoke features (Vicente and Guillemant, 2002; Chen *et al*., 2004; Phillips *et al*., 2000; Yuan *et al*., 2009). Specially, Yuan *et al*. (2009) introduced wavelet transformation into smoke detection in fires, while Chen *et al*. (2004) and Phillips *et al*. (2000) detected smoke by grayish color information and the movement belonging

Corresponding Author: Zhe-Ming Lu, Teaching Building 5, Yuquan Campus, Zhejiang University, 38 ZheDa Road, Hangzhou 310027, People's Republic of China Tel/Fax: +86-571-87951589

to diffusion of particles and detected fires and flames base on the frequency of queasy flames' flicker which is proved to be around 10 Hz (Albers and Agrawal, 1999).

Generally speaking, combining the color, edge and motion information can greatly improve the detection performance. As one of the main features of objects, edge has been used in many fields (Xiang-Wei *et al*., 2009c; Qin *et al*., 2007), so it can be also employed to detect fires (Zhang *et al*., 2008b). In this study, we introduced a new early fire detection system based on the edge and motion features extracted from the flame contours that are determined by the color information.

THE PROPOSED FIRE DETECTION ALGORITHM

In general, typical vision-based fire detection schemes should firstly find out the suspicious or candidate fire frames or regions from the video, where we could further discover the real fire regions based on the motion or edge characters of the candidate regions. In our scheme, we divide the whole fire detection process into three parts, i.e., candidate fire frame selection, flame region selection and flame contour-based fire decision. The candidate fire frame selection stage finds the suspicious frames and removes the unlikely frames based on frame selection rules. The flame region selection step detects the flame pixel points in the candidate fire frames by region selection rules. Finally, flame contour-based fire decision rulers are performed on the flame regions to determine whether a fire occurs in the video or not. These three stages can be illustrated in detail as follows:

Candidate fire frame selection: Generally speaking, a majority of frames in common video are not suspicious ones with fire and flame regions. Because the second and third stages cost much more time, the first stage we should do is to remove unlikely frames as many as possible and only select candidate fire frames as the input of next stage and thus there will be more resource left for further computing and analysis, resulting in a highly efficient and real-time detection system. The flow chart of the candidate frame selection stage is shown in Fig. 1 and can be described as below:

The video to be detected is first segmented into successive frames, F_j, j = 1, 2,…, N. For each frame F_j, we detect each pixel p = (p_R, p_G, p_B) in the frame with the following rule 1 described as Eq. 1.

$$\begin{cases} p \text{ is a fire-colored pixel} & p_R > R_T, p_G > G_T, p_B > B_T \\ p \text{ is not a fire-colored pixel} & \text{otherwise} \end{cases} \quad (1)$$

where, R_T, G_T and B_T are the thresholds of R, G and B components which are defined according to various experimental results, ranging from 120 to 180, 70 to 110 and 30 to 50 respectively. Then we count the number of fire-colored pixels S_j in this frame. Finally, we determine whether the current frame is a fire-colored frame or not by the following rule 2 described as Eq. 2:

$$\begin{cases} F_j \text{ is a fire-colored frame} & S_j > S_T, S_j > S_{j-1} \\ F_j \text{ is not a fire-colored frame} & \text{otherwise} \end{cases} \quad (2)$$

where, S_T is a fire-colored area threshold preset according to various experimental results, which depends on

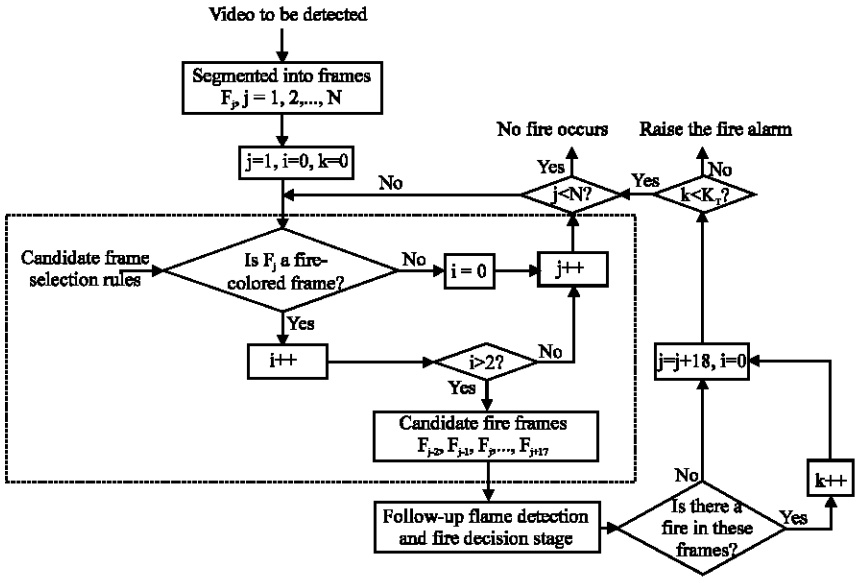

Fig. 1: The flow chart of candidate fire frame selection process in the dashed block

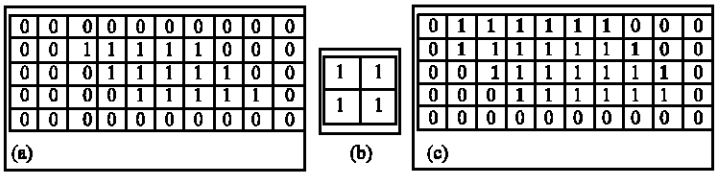

Fig. 2: A concrete dilation example (a) the original image A (b) the set S (c) the image A⊕S

application environments. Obviously, an early fire should be a fire with expanding fire-colored area, so the number of fire-colored pixels in the current frame should be larger than that in the previous frame.

If three consecutive frames F_{j-2}, F_{j-1}, F_j are all selected as fire-colored frames, we select the 20 consecutive frames from F_{j-2} to F_{j+17} as the candidate fire frames for further processing in the follow-up stages. Otherwise, we check next three frames until all frames in the video are processed.

Flame region selection: After obtaining the candidate fire frames, F_j, j = 1, 2,… , 20, we turn to detect accurate flame regions in each candidate frame. For each frame F_j, we check each pixel $p = (p_R, p_G, p_B)$ in this frame and find the flame pixel by the following rule described as Eq. 3:

$$\begin{cases} p \text{ is a flame pixel} & p_R > R_T, p_R > p_G > p_B, p_V \geq (255 - p_R) \cdot V_T / R_T \\ p \text{ is not a flame pixel} & \text{otherwise} \end{cases} \quad (3)$$

where, R_T is the threshold of R component as given in Eq. 1, V_T is the saturation threshold, ranging from 115 to 135 and p_V is the saturation value of the pixel p. Here, the rule $p_R > p_G > p_B$ is derived from the fact that R becomes the major component in a colorful image of fire, whose reason is that the fire is also a light source and the video camera needs sufficient brightness during the night to capture the useful video sequences. Furthermore, to avoid the effect of the background illumination on flame detection, the saturation value of the flame pixel should be larger than a specified threshold, V_T.

Flame contour-based fire decision: Now we come to the key step, i.e., fire decision based on the flame regions we have obtained in the above two steps. In this phase, we will detect whether there is fire in the video or not based on the contour characters of flame regions. This phase can be divided into four steps. First,we convert each candidate frame in the RGB color space into a gray-level image and also a binary image for later use. Second, dilation and erosion operations are performed on each binary image to smooth the image. Third, mini flame regions are removed and small holes in flame regions are filled to improve the efficiency of the edge detector. Finally, we decide whether there is a fire or not based on the contour which is obtained by the canny edge detector. These steps can be described in detail as follows.

For each frame F_j, j = 1, 2,… , 20, we convert it from the RGB color space into a gray-level image GL_j by calculating the gray-level value for each flame pixel while setting each non-flame pixel to be 0 directly. For each pixel $p = (p_R, p_G, p_B)$ in this frame, we get the corresponding gray-level value p_{GL} by Eq. 4:

$$p_{GL} = \begin{cases} 0.59p_R + 0.3p_G + 0.11p_B & p \text{ is a flame pixel} \\ 0 & p \text{ is not a flame pixel} \end{cases} \quad (4)$$

Similarly, the binary image BI_j can be obtained by getting each binary pixel p_{BI} as following Eq. 5:

$$p_{BI} = \begin{cases} 1 & p \text{ is a flame pixel} \\ 0 & p \text{ is not a flame pixel} \end{cases} \quad (5)$$

In experiments, we find that there are small holes and isolated points in the binary image. In order to wipe off these noisy pixels or regions, we further smooth the binary image based on dilation and erosion operations. Dilation and erosion are the basic morphological operators. Dilation of the set A by the set S, denoted by A⊕S, is obtained by first reflecting S about its origin and then translating the result by x. All x such that A and reflected S translated by x that have at least one point in common form the dilated set. It can be described as Eq. 6:

$$A \oplus S = \{x \mid (\hat{S})_x \cap A \neq \varnothing\} \quad (6)$$

where, $\hat{S}$ denotes the reflection of S and $(\hat{S})_x$ denotes the translation of $\hat{S}$. A concrete dilation example is given in Fig. 2. After being processed by the set S given in Fig. 2b, the original image A shown in Fig. 2a is transformed into a new image A⊕S described in Fig. 2c that has more light pixels than the original one.

Similarly, erosion of A by S, denoted as A⊗S, is the set of all x such that S translated by x is completely contained in A, which can be calculated by Eq. 7:

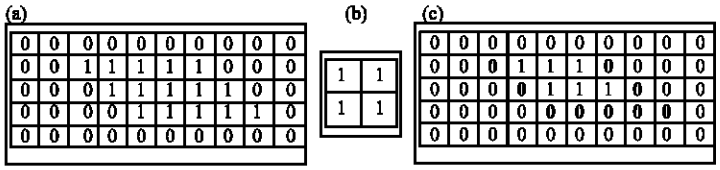

Fig. 3: A concrete erosion example (a) the original image A (b) the set S (c) the image A⊗S

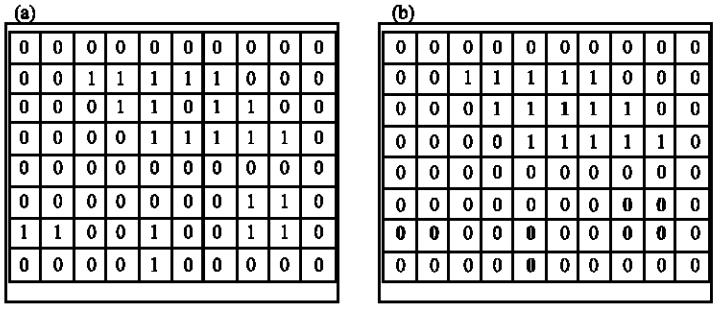

Fig. 4: A concrete mini-region erasing example (a) the original image (b) the image without mini regions

$$A \otimes S = \{x \mid (S)_x \subseteq A\} \tag{7}$$

where, $(S)_x$ denotes the translation of S. A concrete erosion example is shown in Fig. 3. The image A⊗S shown in Fig. 3c derives from the original image A shown in Fig. 3a which is processed by the set S given in Fig. 3b. It is easy to see that the pixels at the edge of the light part have been changed into dark pixels after erosion.

After the above operations, smoothed flame regions in each frame have been obtained. However, there may be some mini regions which will affect the feature calculation and slow down the decision speed. In fact, mini regions are not so important in our decision process, so we can erase them in order to improve the detection efficiency. Here, a simple but effective method is adopted. To remove small flame regions, for every flame region in each frame, the number of flame pixels in this region is first calculated. If the number of flame pixels is less than the preset threshold, then the corresponding region is discarded by setting the pixels in this region to be 0. Otherwise, the region remains unchanged. To fill the small holes in the flame region, for every mini non-flame region surrounded by many flame pixels, similar operations can be performed by setting the pixels in this region to be 1. A concrete example to erase mini regions is shown in Fig. 4. After erasing the mini regions, the original image shown in Fig. 4a is transformed into a new image shown in Fig. 4b that has fewer noisy points than the original one.

Up to now, we have obtained the smoothed flame regions without mini regions. Next we turn to decide if there is a fire in the 20 successive frames by detecting the dynamic features derived from the flame contours. In this study, we get the flame contours based on the Canny edge detector. The main idea of the Canny edge detector is to find edges by searching local maxima of the gradients in an image, where the gradient is calculated with a Gaussian filter. It uses two thresholds for strong and weak edges respectively and the weak edges are accepted if they are connected to the strong ones. With the contours of all flame regions at hand, we can perform fire decision based on the following rule described as Eq. 8:

$$\begin{cases} \text{A fire occurs} & P_S > P_{ST}, P_C > P_{CT}, P_R > P_{RT} \\ \text{No fire occurs} & \text{otherwise} \end{cases} \tag{8}$$

where, P_S, P_C and P_R are the percentages of flame-area-expanding frames, flame-perimeter-expanding frames and frames whose flame roundness is in the predefined range in the whole 20 frames, respectively. P_{CT}, P_{ST} and P_{RT} are predefined thresholds according to various experimental results and they are diverse in different environments. In our experiments, all of them are set to 0.7. P_S can be calculated by following Eq. 9-10:

$$N_j^{(S)} = \begin{cases} 1 & S_j > S_{j-1} \\ 0 & \text{Otherwise} \end{cases} \tag{9}$$

$$P_S = \frac{\sum_{j=1}^{20} N_j^{(S)}}{20} \tag{10}$$

where, S_j is the number of flame pixels in the frame F_j and $N_j^{(s)}$ is the flag denoting whether the number of flame

pixels increases or not compared with its previous frame. Similarly, P_C can be calculated as Eq. 11 and 12:

$$N_j^{(C)} = \begin{cases} 1 & C_j > C_{j-1} \\ 0 & \text{Otherwise} \end{cases} \quad (11)$$

$$P_C = \frac{\sum_{j=1}^{20} N_j^{(C)}}{20} \quad (12)$$

where, C_j is the overall perimeter of all flame contours in the frame F_j, i.e., the number of pixels on the edge of flame contours in the frame F_j. $N_j^{(c)}$ is the flag denoting whether the overall perimeter increases or not compared with its previous frame. In addition, P_R can be calculated as Eq. 13-15:

$$R_j = \frac{(C_j)^2}{4\pi S_j} \quad (13)$$

$$N_j^{(R)} = \begin{cases} 1 & R_{T\min} \le R_j \le R_{T\max} \\ 0 & \text{Otherwise} \end{cases} \quad (14)$$

$$P_R = \frac{\sum_{j=1}^{20} N_j^{(R)}}{20} \quad (15)$$

where, R_j is the overall roundness of all flame contours in the frame F_j and $N_j^{(R)}$ is the flag denoting whether the overall roundness is in the interval $[R_{Tmin}, R_{Tmax}]$ or not. Here, the typical values of R_{Tmin}, R_{Tmax} used in this study are 1.7 and 6, respectively.

Furthermore,it should be mentioned that the distance between the fire source and our camera should range from 3 to 10 m in our scheme, maybe this problem can be solved when multiple cameras are employed in the future study.

It should be noted that, in the whole fire detection system, we may get several candidate fire video segments (each with 20 successive frames), thus we should process them based on the flow chart as shown in Fig. 1. If a candidate fire video segment is judged to be a fire segment, then we add 1 to the counter k. If the counter k is larger than the threshold K_T, then we can definitely raise the fire alarm. If all frames in the video have been processed but k is still less than K_T, then we consider that no severe fire occurs in this video. In fact, we can grade the severity of the fire by using several thresholds for k. Certainly, for various requests in different environments, K_T is different. In our experiments it is set to 1.

EXPERIMENTAL RESULTS AND DISCUSSION

To test the effectiveness of the proposed scheme, we implemented it on a PC with an Intel(R) Core(TM) 2 Duo CPU, 3.16 GHz processor. The software platform is shown in Fig. 5, which is based on Visual C++ 6.0.

In order to show the intermediate results when processing each frame, we pick out an example fire frame as shown in Fig. 6. Figure 6a shows the original example fire frame in the RGB color space. Based on Eq. 4 and 5, we can get the gray-level and binary images as shown in Fig. 6b and c, respectively. After dilation and erosion processing, we can get the smoothed image as illustrated

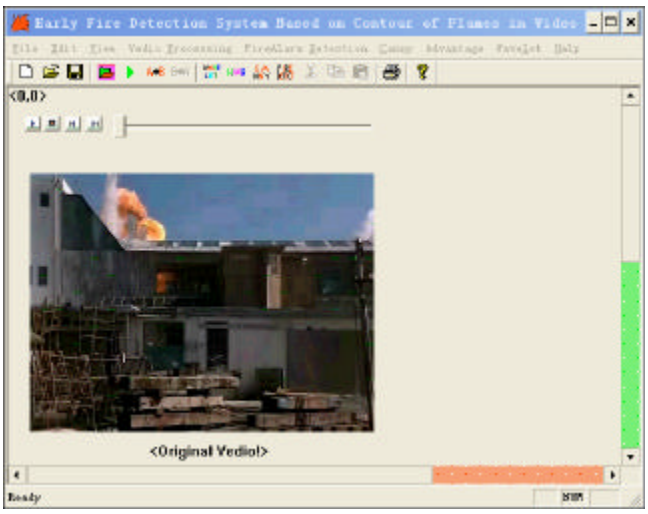

Fig. 5: The software platform

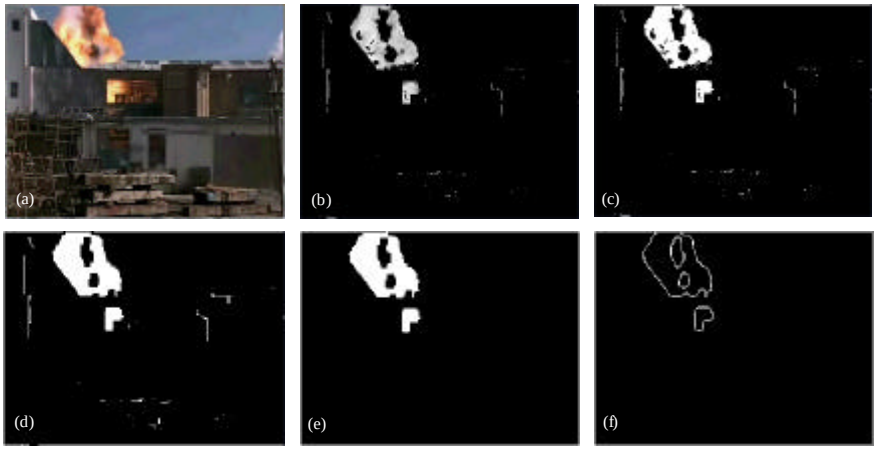

Fig. 6: The intermediate results when processing an example fire frame, (a) original image, (b) grayscale image, (c) binary image, (d) smoothed image, (e) mini-region erased image and (f) flame contours

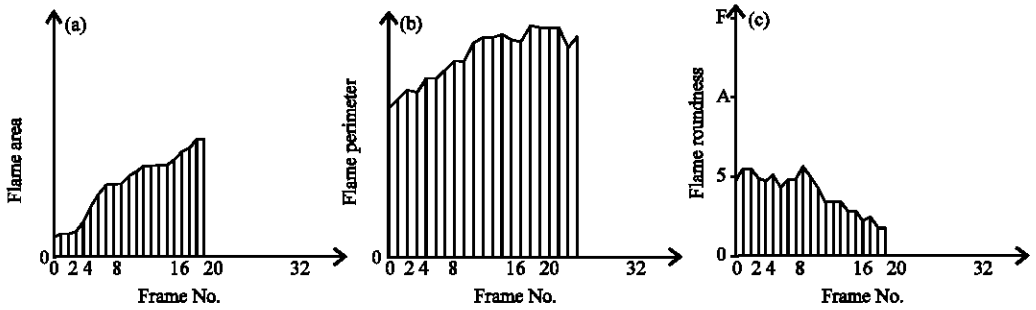

Fig. 7: Parameters S, C and R in an early fire (Frame No.) (a) Area vs. frame No., (b) perimeter vs. frame No. and (c) roundness vs. frame No.

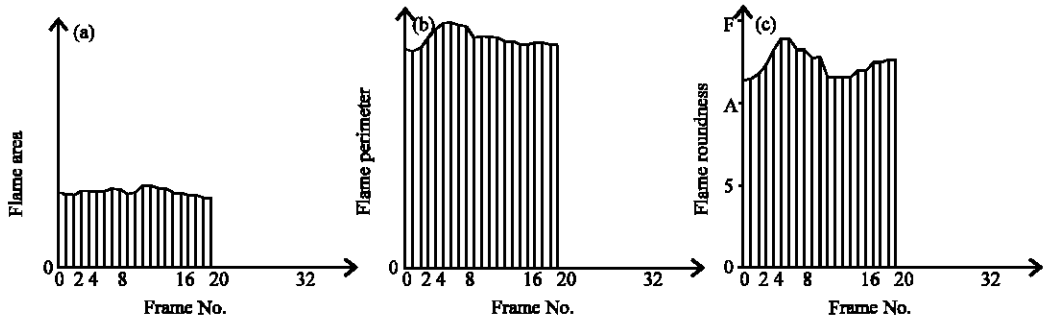

Fig. 8: Parameters S, C and R in the video of a man walking with a firebrand in hand (Frame No.) (a) Area vs. frame No., (b) Perimeter vs. frame No. and (c) Roundness vs. frame No.

in Fig. 6d. After erasing small mini flame regions and filling small mini non-flame regions, we can obtain the mini-region erased image as given in Fig. 6e. Finally, Canny edge detector is performed on Fig. 6e to obtain the flame contours as shown in Fig. 6f. Based on the flame contours in Fig. 6f, we can calculate their features for follow-up fire decision.

Now we turn to show the effectiveness of the three parameters, S_j, C_j and R_j used in the fire decision stage. Here, four cases are tested and their results are shown in Fig. 7-10, respectively. In the first case, an early fire video clip is input into our system and Fig. 7a-c show the changes in flame areas, flame perimeters and flame roundness as time goes on, respectively. We can find that

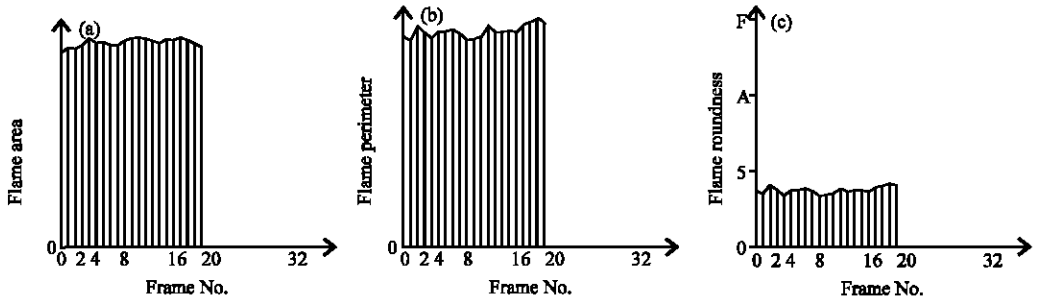

Fig. 9: Parameters S, C and R in an interim fire (Frame No.) (a) area vs. frame No., (b) perimeter vs. frame No. and (c) roundness vs. frame No.

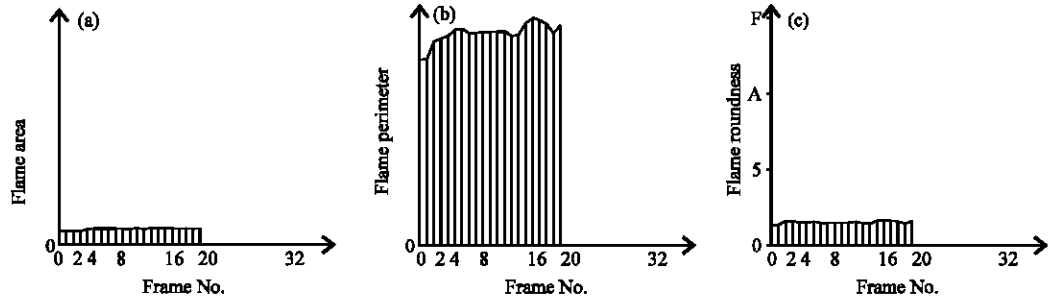

Fig. 10: Parameters S, C and R in the fire within a vessel which is far from the camera (40 m) (Frame No.) (a) area vs. frame No., (b) perimeter vs. frame No. and (c) roundness vs. frame No.

the flame area increases rapidly as time goes on for an early fire. Furthermore, the flame perimeter also increases at the beginning of a fire. In addition, the flame roundness ranges from 1.8 to 5.3. That is to say, Eq. 8 is effective in detecting an early fire. In the second case, our system is used to detect the fire lighted by a man walking slowly with a firebrand in hand and the result is shown in Fig. 8. Figure 8a indicates that the flame area in each frame is almost kept unchanged, thus the decision rule with respect to flame areas doesn't work for this case. Similarly, from Fig. 8b and c, we can see that the decision rules with respect to flame perimeters and roundness don't work for this case either. In the third case, we would like to check the effect of our detection system on an interim fire and the result is shown in Fig. 9. As shown in Fig. 9c, the rule with respect to roundness is still satisfied for an interim fire. However, from Fig. 9a and Fig. 9b, we can clearly see that both the flame area and the flame perimeter are steady, thus the two corresponding rules are not satisfied. Therefore, it is our future work to deal with such a fire. In the last case, we would like to test an extreme condition where the fire is in a vessel far from the camera (nearly 40 m) and the result is shown in Fig. 10. Figure 10a points out that the rule with respect to flame areas is not obeyed and Fig. 10b shows that the rule with respect to flame perimeters is not satisfied either. From Fig. 10c, we can see that the roundness is nearly kept unchanged around 1.5, which is less than $R_{tmin} = 1.7$. Thus, none of the three rules are satisfied for such an extreme case. In fact, if the video clips from multiple cameras can be obtained, maybe this problem can be solved.

In order to compare with other schemes in the aspect of extracting flame regions and contours, we select three fire frames to test the excellence of our flame pixels extraction step compared with (Cho *et al*., 2008) scheme and the superiority of our contour extraction step to (Xu *et al*., 2008) scheme. The results are shown in Fig. 11 and 12, respectively. Figure 11a, d and g are the three original fire frames, Fig. 11b, e and h are flame regions obtained by Cho *et al*. (2008) scheme, Fig. 11c, f and i are flame regions obtained by our scheme. From these results, we can see that our scheme can obtain clearer and smoother flame regions without noisy points. And Fig. 12a, d and g are the three original fire frames which are the same as the frames in Fig. 11a, d and g, Fig. 12b, e and h are flame contours obtained by Xu *et al*. (2008) scheme, Fig. 12c, f and i are flame contours obtained by our scheme. From these results, we can see that our scheme can obtain clearer contours without noisy points. From above experimental results and in comparison with Cho *et al*. (2008) scheme and Xu *et al*. (2008) scheme, it is obvious to find out that our scheme can get

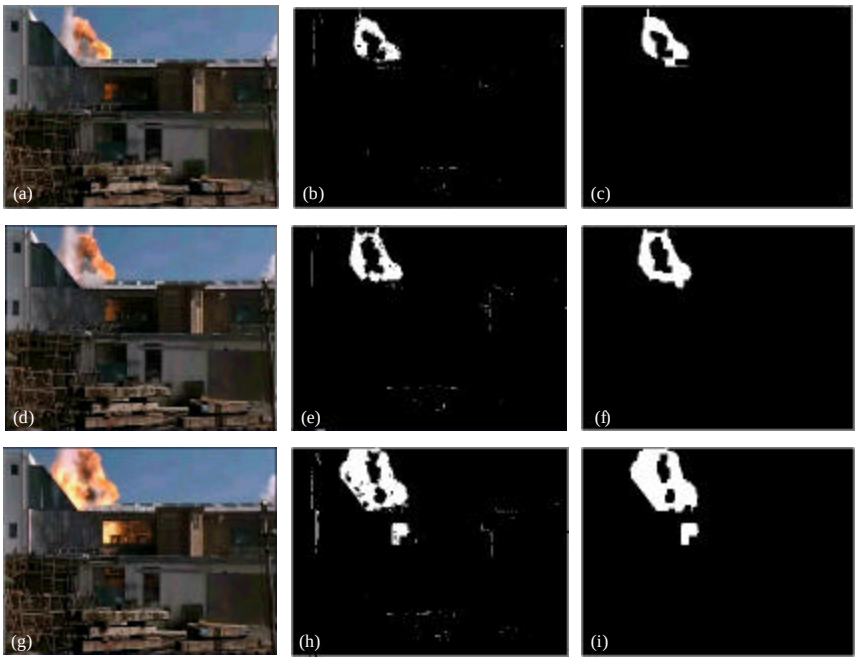

Fig. 11: The flame regions extracted by Cho *et al*. (2008) scheme and our scheme (a) Original frame 1, (b) flame regions by Cho *et al*. (2008) scheme, (c) flame regions by our scheme, (d) original frame 2, (e) flame regions by Cho *et al*. (2008) scheme, (f) flame regions by our scheme, (g) Original frame 3, (h) Flame regions by Cho *et al*. (2008) scheme and (i) flame regions by our scheme

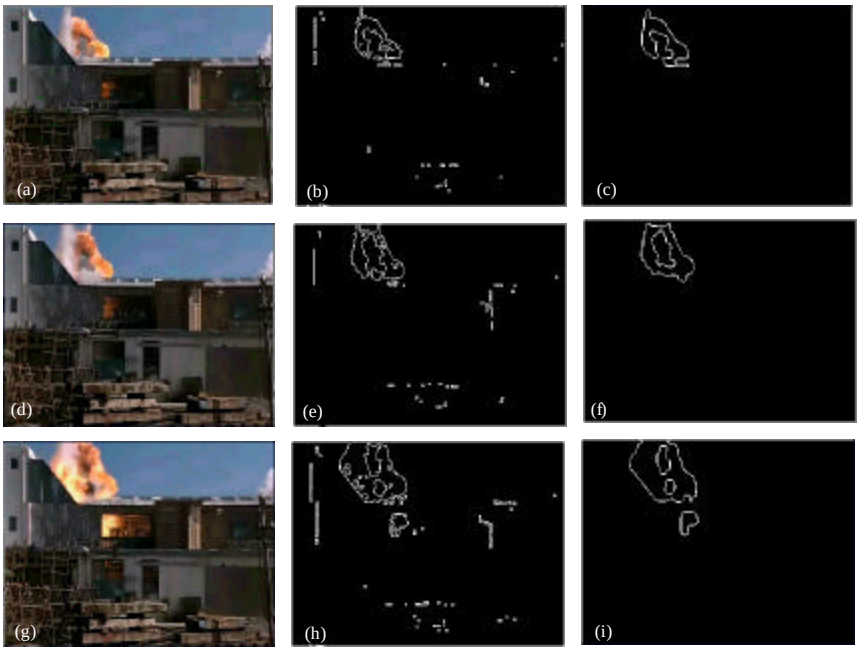

Fig. 12: The flame contours extracted by Xu *et al*. (2008) scheme and our scheme (a) original frame 1, (b) flame contours by Xu *et al*. (2008) scheme, (c) flame contours by our scheme, (d) original frame 2, (e) flame contours by Xu *et al*. (2008) scheme, (f) flame contours by our scheme, (g) original frame 3, (h) flame contours by Xu *et al*. (2008) scheme and (i) Flame contours by our scheme

smootherflame regions and clearer flame contours in each frame and there are also almost no contours of mini flame regions left in the image in our scheme. These advantages and improvements lead to more efficiency and veracity in calculation of the area, the perimeter and the roundness of flame contour for fire detection, resulting in high efficiency and real time of fire alarm detection. Therefore, we can conclude that our method can provide effective detection results for early fires, but there are also some limitations and disadvantages in our scheme. For example, when the fire grows up into interim fire, our scheme is no longer efficient to detect the fire because the characters of flames we give are not enough. And when the fire is far from our camera, our scheme don't work either, maybe in the future study the indraught of multiple-view video can solve this problem. So for more wide use, there is much more work required to be done in the future.

CONCLUSIONS AND FURTHER WORK

This study presents an early fire detection system based on flame contours in the video. Three rules for candidate fire frame selection, flame region selection and flame contour-based fire decision are designed in detail. Dilation, erosion and mini region erasing operations are introduced in the preprocessing of flame regions. Canny edge detector is performed on smoothed flame regions to obtain the flame contours. Three parameters, i.e., area, perimeter and roundness, related to flame contours are introduced in fire decision. Extensive experiments have been performed to test the effectiveness of the proposed algorithm for early fire detection. Future work will be concentrated on: (1) Application of the improved method to multiple-view video clips to improve the detection accuracy. (2) Introduction of more characters of flame contours and more detection rules in fire decision, especially for an interim fire. (3) Fire detection in 3D video clips instead of 2D video clips.

REFERENCES

Albers, B.W. and A.K. Agrawal, 1999. Schlieren analysis of an oscillating gas-jet diffusion flames. Combust. Flame, 119: 84-94.

Celik, T., H. Ozkaramanli and H. Demirel, 2007. Fire pixel classification using fuzzy logic and statistical color model. Proc. IEEE Int. Conf. Acoustics Speech Signal Process., 1: 1205-1208.

Chen, T., P. Wu and Y. Chiou, 2004. An early fire-detection method based on image processing. Proc. Int. Conf. Image Process., 3: 1707-1710.

Cho, B.H., J.W. Bae and S.H. Jung, 2008. Image processing-based fire detection system using statistic color model. Proceedings of the International Conference on Advanced Language Processing and Web Information Technology, July 23-25, Dalian Liaoning, China, pp: 245-250.

Healey, G., D. Slater, T. Lin, B. Drda and D. Goedeke, 1993. A system for real-time fire detection. Proceedings of the Computer Vision and Pattern Recognition, June 15-17, New York, USA., pp: 605-606.

Horng, W.B., J.W. Peng and C.Y. Chen, 2005. A new image-based real-time flame detection method using color analysis. Proceedings of the International Conference on Networking, Sensing and Control, March 19-22, University Marriott Park Hotel, Tucson, USA., pp: 100-105.

Jin, H. and R.B. Zhang, 2009. A fire and flame detecting method based on video. Proc. 8th Int. Conf. Mach. Learn. Cybernet., 4: 2347-2352.

Phillips III, W., M. Shah and N.V. Lobo, 2000. Flame recognition in video. Proceedings of the 5th IEEE Workshop on Applications of Computer Vision, Dec. 4-6, Palm Springs, CA, USA., pp: 224-229.

Qin, Z., J. Jia, T.T. Li and J. Lu, 2007. Extracting 2D projection contour from 3D model using ring-relationship-based method. Inform. Technol. J., 6: 914-918.

Toreyin, B.U., Y. Dedeoglu and A.E. Cetin, 2005. Flame detection in video using hidden markov models. Proc. IEEE Int. Conf. Image Process., 2: 1230-1233.

Toreyin, B.U., Y. Dedeoglu, U. Gueduekbay and A.E. Cetin, 2006. Computer vision based method for real-time fire and flame detection. Pattern Recognition Lett., 27: 49-58.

Vicente, J. and P. Guillemant, 2002. An image processing technique for automatically detecting forest fire. Int. J. Therm. Sci., 41: 1113-1120.

Xiang-Wei, L., Z. Ming-Xin, Z. Geng-Lie, Z. Ya-Lin and Z. Shuang-Ping, 2009a. Effective video analysis preprocessing algorithm based on rough sets in compressed domain. Res. J. Inform. Technol., 1: 51-56.

Xiang-Wei, L., M.X. Zhang, S.P. Zhao and L.Y. Zhu, 2009b. A novel dynamic video summarization approach based on rough sets in compressed domain. Inform. Technol. J., 8: 388-392.

Xiang-Wei, L., L. Zhan-Ming, Z. Ming-Xin, Z. Ya-Lln and W. Wei-Yi, 2009c. Rapid shot boundary detection algorithm based on rough sets in video compressed domain. Res. J. Inform. Technol., 1: 70-78.

Xu, Z.G. and J.L. Xu, 2007. Automatic fire smoke detection based on image visual features. Proceedings of the International Conference on Computational Intelligence and Security Workshops, Dec. 15-19, Harbin, Beijing, pp: 316-319.

Xu, X.J., Y. Shao and S.F. Guo, 2008. Edge detection operators and their application in flame image. Control Automat., 24: 313-314.

Yu, F.X., J.Y. Su, Z.M. Lu, P.H. Huang and J.S. Pan, 2008. Multi-feature based fire detection in video. Int. J. Innovative Comput. Inform. Control, 4: 1987-1993.

Yuan, W., C. Yu and Y. Zhang, 2009. Based on wavelet transformation fire smoke detection method. Proceedings of the 9th International Conference on Electronic Measurement and Instruments, Aug. 16-19, Beijing, China, pp: 872-875.

Zhang, D., J. Zhao, J. Zhao, S. Han, Z. Zhang, C. Qu and Y. Ke, 2008. A new color-based segmentation method for forest fire from video image. Proceedings of the International Seminar on Future BioMedical Information Engineering, Dec. 18, Wuhan, Hubei, China, pp: 41-44.

Zhang, Z., J. Zhao, D. Zhang, C. Qu, Y. Ke and B. Cai, 2008. Contour based forest fire detection using FFT and wavelet. Proc. Int. Conf. Comput. Sci. Software Eng., 1: 760-763.